Conditions for static friction between flat crystalline surfaces

Martin H. Müser

Institut für Physik, Johannes Gutenberg Universität, 55099 Mainz, Germany

Mark O. Robbins

Department of Physics and Astronomy, Johns Hopkins University, Baltimore, Maryland 21218

(Received 15 June 1999)

The conditions for the presence of static friction between two atomically smooth crystalline surfaces are investigated. Commensurate and incommensurate walls are studied. While two commensurate walls always pin at zero lateral force and positive pressures, incommensurate walls only pin if mobile atoms are present in the interface between the surfaces or if the solids are particularly soft. Surprisingly, static friction can be observed between rigid surfaces, either commensurate or incommensurate, that are separated by a freely diffusing fluid layer.

I. INTRODUCTION

Recent studies have revealed interesting transitions in the shear response of many fluids when they are confined between crystalline surfaces that are only a few nanometers apart.[1–10] Even though thick films are simple fluids at the imposed pressure and temperature, a yield stress or static friction is observed when the film thickness is decreased to a few molecular diameters. This is generally assumed to reflect a transition to a solid-like state of the film due to the bounding walls. In some experiments there is a continuous divergence of the viscosity and relaxation time that is typical of a bulk glass transition.[9] Other experiments show a sharp onset of the yield stress that is more akin to a first-order liquid to crystal phase transition.[10] Simulations have found both types of transition depending on factors such as the relative size of wall and fluid atoms and the molecular structure of the fluid.[4,5] They also reveal that solid films transform back into a fluid state when the yield stress is exceeded, explaining the stick-slip motion observed in some experiments.[2,11]

There is, however, an important difference between most simulations[1–6] and experiments.[7–10] Surfaces used in computer simulations are typically commensurate, i.e., share common periodicities. In fact, most simulations use identical, aligned crystals for the two walls. Many also set the number of atoms between the surfaces to an integer multiple of the number of atoms in one surface layer, facilitating the formation of ideal crystals. This cannot reflect typical experiments—even those between nominally identical surfaces. The reason is that the crystallographic orientation of the surfaces is rarely controlled, and any small orientational misfit between otherwise identical surfaces makes them incommensurate.[12,13] There is no well-defined crystalline state of the film that can simultaneously lock into registry with two incommensurate surfaces. Some of the interactions between the wall and fluid atoms must be frustrated, and the dynamics and statistical properties of the system may be altered qualitatively due to this frustration.

The contrast between commensurate and incommensurate cases can be illustrated by considering a submonolayer film of molecules between two identical crystalline surfaces in the limit of high confining pressures where the hard-sphere interactions between wall and film atoms dominate. If the surfaces are aligned and translated so that all surface atoms are directly above each other, they create a periodic array of large openings that can accommodate film molecules. Any relative displacement of the commensurate walls greatly reduces the volume of these openings and is resisted by the hard-sphere repulsion between wall and film atoms. This can be expected to prevent translation of one wall relative to the other until a yield stress is exceeded. Note that individual film molecules should still diffuse freely because there is a finite activation energy for motion between openings. This diffusion does not affect the equilibrium positions of the walls because all openings are equivalent.

The situation is very different when the walls are made incommensurate by a relative rotation. Because the walls share no common periodicity, all possible relative positions of atoms on the two surfaces are sampled with equal probability. Each opening is slightly different and all displacements of the walls produce the same distribution of openings. It is well known that this symmetry under translation can lead to a vanishing yield stress and free diffusion of the walls in the absence of a thin intervening film.[12,13] However, recent computer simulations[14] indicate that a film can pin incommensurate surfaces together, providing a natural explanation for the observation of static friction in experiments.

The simple picture for submonolayer films is that molecules search out the best set of openings for the given wall positions. They then resist translation of the walls because these openings will be constricted by any translation. Although there is an equivalent set of openings after translation, these may be far away and only reached via a complex, coordinated reshuffling of the molecules with a large activation free energy.

This type of pinning is much more subtle than that between commensurate walls, and one may wonder whether it persists in the thermodynamic limit. For example, diffusion of individual molecules necessarily takes them to inequivalent openings where they produce a different force on the walls. This will lead to a small displacement of the walls in any finite system, and accumulated motion of individual film

     PRB <u>61</u>   2335

molecules might cause gradual diffusion of the walls that remains relevant in the thermodynamic limit.

In this paper we will investigate the conditions that determine whether two surfaces are pinned together in the thermodynamic limit. The most sensitive technique is to consider the case where no force is applied in the direction tangential to the walls, and to measure the relative displacement of the walls as a function of time. Finite systems will always show diffusion at sufficiently long times due to thermal activation, just as the magnetic moment of finite systems will always change sign. Hence it is crucial to consider the scaling of the mobility of the walls with system size in order to determine the behavior in the thermodynamic limit.

We present results for commensurate and incommensurate walls as a function of temperature and normal pressure. In each case we compare results for bare walls to results for walls separated by a submonolayer film. We find that both commensurate and incommensurate walls remain pinned even when the film molecules diffuse freely. One may expect that incommensurate walls undergo a transition from pinned to unpinned with increasing temperature or decreasing pressure, but it is difficult to identify the transition with available system sizes. A general argument is presented that commensurate walls are always pinned even as the film becomes a nearly ideal gas, although the pinning force may become exponentially small. Thus observation of static friction between two commensurate crystals need not imply that the intervening film is solid as is often assumed.

In the next section we describe the model used in the simulations and the averaging techniques. Section III presents results for commensurate and incommensurate walls, with and without monolayer films. Our conclusions are summarized in Section IV.

II. METHOD

In this study, we have used the same model as in Ref. 14. The walls are [111] surfaces of an fcc crystal, and therefore have a triangular lattice structure. Atoms in the walls are coupled to their equilibrium lattice sites by springs of stiffness κ. In the limiting case of rigid walls, the coupling is considered infinitely strong, $\kappa = \infty$, and the atoms are constrained to their equilibrium positions. Periodic boundary conditions are applied in the plane of the walls. The coordinate system is chosen so that $\hat{x}$ and $\hat{y}$ are in the plane of the walls and $\hat{z}$ is normal to them.

The molecules between the walls are short chains, each containing six monomers. All monomers interact with each other and with wall atoms via a truncated Lennard-Jones potential,

$$V(r) = 4\epsilon[(\sigma/r)^{12} - (\sigma/r)^6] + V_c, \qquad (2.1)$$

where r is the separation, and ϵ and σ are characteristic energy and length scales, respectively. Wall atoms from opposing surfaces interact via the same Lennard-Jones potential. The potential is cut off at r_c and shifted by V_c so that $V(r_c) = 0$. Adjacent monomers on a chain interact via an additional FENE potential[15]

$$V_{CH}(r) = -(1/2)kR_0^2 \ln[1 - (r/R_0)^2], \qquad (2.2)$$

where $R_0 = 1.5\sigma$ and $k = 30\epsilon/\sigma^2$. All quantities are expressed in units of σ, ϵ, and the mass m of one monomer. The characteristic time is $t_{LJ} \equiv \sqrt{m\sigma^2/\epsilon}$. Unless stated otherwise, $r_c = 2^{1/6}\sigma$.

The lattice sites of the bottom wall are fixed, while the top wall is allowed to move under the combined influence of the force from the coupling springs and an external force on each lattice site $\vec{f}$. A constant external force f_z is applied normal to the top wall, and the tangential components of the external force $\vec{f}_\parallel$ are set to zero to allow free diffusion in the plane of the walls. We choose a mass of the top wall M_w that is only half the combined mass of one layer of atoms. This choice allows the top wall to respond more rapidly than if we choose a more physical mass of several layers. Transition state theory and corrections to it show that the rate at which energy barriers are crossed scales as $\sqrt{1/M_w}$ to leading order.[16] By using a lighter mass we speed the calculations without changing the qualitative behavior.

Both the diffusion of the top wall and the diffusion of individual monomers are monitored. The mean-squared displacements along $\hat{x}$ and $\hat{y}$ are calculated separately, and then averaged to get $\langle \delta x^2(t) \rangle$, the mean-squared displacement along a single coordinate after a time t. The results are also averaged over at least eight independent intervals of length t.

The equations of motion are integrated using a fifth-order predictor-corrector method with time step $\Delta t = 0.005 t_{LJ}$. The temperature T is controlled by coupling the monomers, and wall atoms if mobile, to a Langevin thermostat.[17] The frictional force in the Langevin equation is $-\gamma m\mathbf{v}$ where $\mathbf{v}$ is the instantaneous velocity and γ is the damping rate. We use $\gamma = 2 t_{LJ}^{-1}$ so that the motion of the particles is well into the underdamped regime. A small additional damping with rate 0.05γ was added to the center of mass of the top wall. These dampings fix the free diffusion of the top wall in the absence of any interactions with the bottom wall at $D_0 = k_B T/2.05\gamma M_w$, where k_B is Boltzmann's constant. Note that the denominator gives the ratio of damping force to velocity for uniform motion of the top wall.

III. RESULTS

We will present results for the simplest choices of commensurate and incommensurate walls. In all cases the top and bottom walls have the same structure and nearest-neighbor spacing, $d = 1.209\sigma$. The size of the surfaces will be expressed in terms of the number N of atoms per layer of wall atoms. The area A is given by $A = N\sqrt{3}d^2/2$. Thus to convert between the force on each atom and a pressure or shear stress, values of $\vec{f}$ should be divided by $1.266\sigma^2$.

In the commensurate case the walls are perfectly aligned, as if a single crystal had been cut in two at the interface. The incommensurate case corresponds to rotating the top wall by 90° relative to the bottom wall. However, the walls must also be distorted slightly in order to conform to the same periodic boundary conditions. This means that the walls are not truly incommensurate, but the residual commensurability does not appear to influence the results. As discussed below, the amount of the distortion and the difference from ideal incommensurate surfaces decrease with increasing system size.

For each choice of walls we will first consider the limiting

case of rigid walls with no molecules in between. Then the constraint of rigidity is relaxed, and finally molecules are introduced between the surfaces. The presence of a sub-monolayer film is enough to move the walls far enough apart that there are no direct interactions between them. Any pinning must be mediated through interactions with the film.

The key question is to determine whether there is a potential that pins the lateral position of the top wall relative to the bottom wall. We define the following time-dependent measure $\tilde{D}(t)$ for the mobility of the top wall at time t:

$$\tilde{D}(t) = \frac{\langle \delta x^2(t) \rangle}{2tD_0}, \tag{3.1}$$

where D_0 is the free diffusion constant of the top wall and is included to remove the trivial decrease in diffusion due to increasing wall mass as N increases. The top wall is pinned if

$$\tilde{D} = \lim_{t \to \infty} \lim_{N \to \infty} \tilde{D}(t) \tag{3.2}$$

tends to zero. If $\tilde{D}$ remains finite, the wall is unpinned and the product $\tilde{D}D_0$ can be interpreted as the long time diffusion constant of the top wall.

A. Commensurate walls

1. Bare surfaces

If the surfaces are infinitely rigid, the only degrees of freedom are associated with the location of the center of mass of the top wall. Each atom on the surface of the top wall ''feels'' exactly the same potential and force from atoms in the bottom wall. The total force on the center of mass coordinate is a periodic function of the lateral displacement that grows linearly with N. In the thermodynamic limit, an infinite activation energy is needed to displace the wall and there can be no diffusion.

Relaxing the constraint of infinite rigidity does not change the linear scaling of activation energy with N, although it may lower the prefactor. In our system, decreasing κ allows atoms to translate relative to the center of mass coordinate in order to lower their energy. There is no change in the ground state energy, but the energy of transition states is decreased. At finite temperature, thermal displacements further decrease the activation free energies. Due to the strictly harmonic nature of the springs, the motions of the independent atoms add incoherently to yield a single effective Langevin noise and damping term on the center of mass. Thus the problem maps into diffusion of a single, damped particle in a periodic potential U, where U depends on the temperature, pressure, and κ.

Diffusion in a periodic potential has been studied in great detail by a number of authors.[18,19] The general trends are illustrated by the results for the simple case of diffusion of a particle in a one-dimensional sinusoidal potential with activation energy ΔF. In this case the diffusion constant satisfies[18]

$$D = D_0[I_0(\Delta F/2k_BT)]^{-2} \tag{3.3}$$

where I_0 is the modified Bessel function. When $\Delta F/2k_BT$ is small, the particle diffuses almost freely:
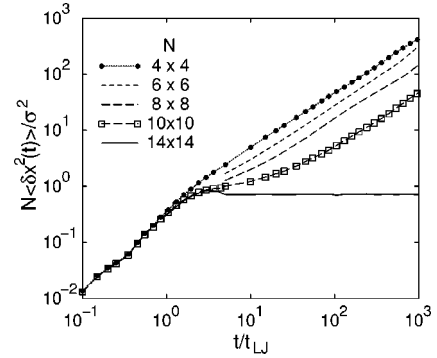

FIG. 1. Mean-squared displacement of top wall along a single coordinate, $\langle \delta x^2(t) \rangle$, as a function of time t for commensurate walls of the indicated sizes. Displacements are multiplied by N to remove the trivial dependence on wall mass. Here $f_z = 1.2\epsilon/\sigma$ and $k_BT = 0.8\epsilon$.

$$D \approx D_0[1 - (\Delta F/k_BT)^2/8]. \tag{3.4}$$

In the opposite limit $\Delta F/2k_BT \gg 1$, the diffusion is activated:

$$D \approx D_0(\Delta F/2k_BT)\exp(-\Delta F/k_BT). \tag{3.5}$$

Since ΔF increases linearly with the area of the wall, the motion will always be activated for large enough system sizes, and will vanish exponentially in the thermodynamic limit. However, one may need very large system sizes to reach this limit for reasonable parameters.

Figure 1 shows the mean-squared displacement of the top wall $\langle \delta x^2(t) \rangle$ as a function of time for $f_z = 1.2\epsilon/\sigma$, $k_BT = 0.8\epsilon$, and the indicated wall sizes. The mean-squared displacements are multiplied by N to remove the trivial dependence on wall mass. This collapses the data at early times, where the walls move ballistically $\langle \delta x^2(t) \rangle \propto t^2$. At longer times the smallest system shows a simple crossover to diffusive motion, $\langle \delta x^2(t) \rangle = 2Dt$. The value of the diffusion constant is nearly equal to the value for free diffusion, D_0. As N increases, a plateau develops between the ballistic and diffusive regions, and the diffusion constant decreases. By $N = 144$ the wall is completely pinned over the length of the simulation, although any finite system will eventually diffuse. These results are just what would be expected from Eq. (3.3) with $\Delta F \propto N$. For small systems, $\Delta F/2k_BT$ may be so much less than unity that free diffusion is observed. However as N increases, the motion becomes activated, and D drops precipitously.

Figure 2 illustrates this behavior for a number of normal forces. The diffusion constant is plotted as a function of the number of atoms in a wall layer N for $\kappa = 100\epsilon\sigma^{-2}$ and $k_BT = 0.8\epsilon$. The free diffusion constant D_0 is indicated by a solid line. In each case, D was evaluated from the time t_1 to diffuse a distance σ along one of the coordinates parallel to the walls using the relation $D = \sigma^2/2t_1$.

At the lowest f_z and N, D decreases roughly as $1/N$ and is nearly equal to the value for free diffusion. As N increases, there is a rapid drop in D, indicating a crossover to activated behavior. The success of Eq. (3.3) in describing this crossover is illustrated by fits to the results for $f_z = 0.1$ and $0.3\epsilon/\sigma$ (broken lines). Increasing f_z moves the crossover to activated behavior to lower N, indicating that ΔF rises with f_z as well as N. This is entirely consistent with the linear relation
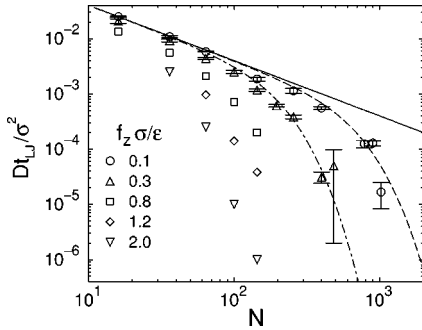
FIG. 2. Diffusion constant calculated from the time to move by σ as a function of the number of atoms per wall N at the indicated values of $f_z\sigma/\epsilon$ and $k_BT=0.8\epsilon$. A solid line shows the free diffusion constant D_0. Dashed and dot-dashed lines show fits to Eq. (3.3) for $f_z=0.1$ and $0.3\epsilon/\sigma$, respectively.

FIG. 3. Mean-squared displacement along a single coordinate, $\langle \delta x^2(t)\rangle$, of individual monomers and of top wall as a function of time t at $f_z=10\epsilon/\sigma$ and $k_BT=0.8\epsilon$. The walls are commensurate and $N=32\times32$.

between static friction and pressure that is found for commensurate surfaces[20] and for incommensurate surfaces separated by adsorbed layers.[14]

The main lesson to be learned from Fig. 2 is that while it is easy to determine that a system is pinned, there is no simple way to prove that a system is unpinned in the thermodynamic limit. Relatively large systems can appear to diffuse freely, even under conditions where systems become pinned in the thermodynamic limit. The reason is that the activation energy for $f_z=0.1\epsilon/\sigma$ is small, which is due to the large average distance between the walls $\langle\Delta z\rangle=1.214$. This value exceeds the value for the interaction cutoff radius of $r_c=2^{1/6}$. Thus the probability of an atom in the top wall having a nonzero interaction with the bottom wall at any given instant is very small.

2. Submonolayer lubrication

The two commensurate walls considered here contain 32×32 atoms in each surface. The film in between consists of 42 chain molecules each containing six monomers. This corresponds to 1 monomer for every 4 atoms on each wall, and is roughly 1/4 of an equilibrium monolayer. The bottom wall is fixed and the normal force on each atom in the top wall $f_z=10\epsilon/\sigma$. This corresponds to a normal pressure $p_z=7.96\epsilon/\sigma^3$. The tangential force $\vec{f}_\parallel=\vec{0}$, and $k_BT=0.8\epsilon$. For comparison, we note that the triple point of monomers with long-range interactions ($r_c\to\infty$) is at $k_BT=0.7\epsilon$.

In Fig. 3, the motion of the top wall is compared to the motion of individual monomers in the chain molecules. The interpretation of the dynamics of the monomers in Fig. 3 is as follows. For times $t<5\times10^{-2}t_{LJ}$ the monomers are in the ballistic regime $\langle\delta x^2(t)\rangle\propto t^2$. For times $0.5<t/t_{LJ}<10^3$, the monomers exhibit subdiffusive behavior that indicates they are initially trapped near a single energy minimum in the periodic potential provided by wall atoms.[21] At $t=10^3 t_{LJ}$, a monomer has typically moved 1σ, which approximately corresponds to the distance between two equivalent minima in the periodic potential. At longer times the motion of the monomers approaches diffusive behavior, where the mean-squared displacement grows linearly with time. Thus the monomers act like particles in a lattice gas, hopping between minima in the wall potential.

During the entire length of this simulation the top wall remained stuck in one minimum and no diffusive behavior
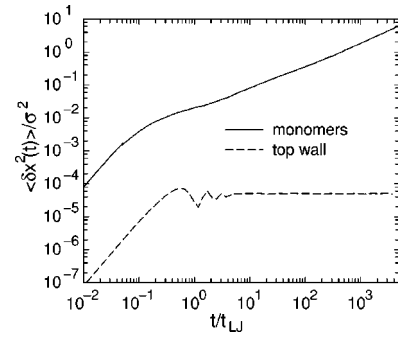
could be observed. Oscillations around the equilibrium position led to a mean-squared displacement that saturated at $5.0\times10^{-5}\sigma^2$. This and the temperature can be used to estimate the effective spring constant for the local free energy minimum of $\kappa_{\rm eff}=15.6\epsilon/\sigma^2$ per wall atom. An estimate of the static friction F_s in the x direction can then be obtained if one makes the simplest assumption for the form of the periodic variation of free energy with x, leaving y unconstrained. The period is given by the distance along x to the nearest equivalent minimum. For a triangular surface this is half of the nearest-neighbor spacing d. Using a single Fourier component to represent the free energy we have $\widetilde{F}(x)=-\widetilde{F}_1\cos(4\pi x/d)$. The static friction is given by the maximum force, i.e., the maximum of the first derivative of $\widetilde{F}$. The maximum of the second derivative gives $\kappa_{\rm eff}$. Using this and the value of $\kappa_{\rm eff}$ from above, we obtain $F_s=\kappa_{\rm eff}d/4\pi=1.5\epsilon/\sigma$. This agrees quite well with the actual friction force of $F_s\approx1.4\epsilon/\sigma$ that we obtained in an independent run. However, we note that our arguments are too rough to expect this level of agreement, because geometrical factors and higher harmonics in the free energy have been left out.

The walls never approached close enough to interact *directly*. Hence, the pinning of top and bottom wall was mediated by the film in between, which was freely diffusing in a lattice-gas-like state. This result may seem rather counterintuitive. The observation of a yield stress in surface force apparatus experiments[7–10] is often assumed to imply that the thin film confined between the surfaces has entered a solid state. This clearly need not be the case *if* the two surfaces are aligned into a commensurate configuration. More generally, the ability of crystals to resist shear does not depend on a lack of diffusion, but rather the presence of long-range order that produces Bragg peaks. In certain crystals, e.g., ionic conductors, the diffusion of some species can be quite rapid. As long as the density modulation measured by the Bragg peaks remains, the system can resist shear.

A simple argument shows that two commensurate walls should be pinned in the thermodynamic limit at all T and f_z. The reason is that the periodic potential of a single wall induces a commensurate density modulation parallel to the wall in an adjacent film.[22] The magnitude of the density modulation will decrease exponentially with distance from the wall, but remains finite. If there is a commensurate wall at some distance h, the energy will necessarily depend on the
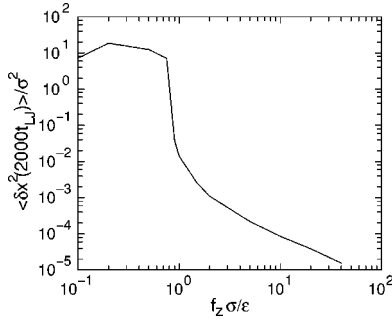
FIG. 4. Mean-squared displacement of top wall along a single coordinate, $\langle \delta x^2(t) \rangle$, after time $t = 2000 t_{LJ}$ as a function of f_z at $k_B T = 0.8 \epsilon$. The walls are commensurate and $N = 32 \times 32$.

registry between the density modulation and the wall lattice. Thus there will always be a periodic force that pins the wall and that grows linearly with system size. However, the free energy barrier ΔF will decrease exponentially with h, and the size of the system must increase proportionately in order to reach the thermodynamic limit. Our conclusions are consistent with simulations by Curry *et al.*,[6] who considered films that were several layers thick and found a periodic pinning force even when there was rapid diffusion within the film.

Figures 4 and 5 show that simulations with a *fixed* system size exhibit an *apparent* transition from pinned to depinned as f_z decreases or T increases. The mean-squared displacement after $2000 t_{LJ}$ is plotted as a function of f_z or T. At low f_z or high T the mean-squared displacement is consistent with the value for free diffusion, $\langle \delta x^2 \rangle \approx 10 \sigma^2$. Thus for these parameters and at this system size ΔF is much less than $k_B T$ [Eq. (3.3)]. However, as noted for dry commensurate walls, this is not enough to establish that the system remains unpinned in the thermodynamic limit. If ΔF diverges in the limit $N \to \infty$, the system will be pinned in the thermodynamic limit. Our results are consistent with $\Delta F \propto N$ at all f_z and T. Simulations with larger N show a consistent shift of the apparent transition to free diffusion to lower f_z and higher T.

B. Incommensurate walls

1. Bare surfaces

Models of the friction between two surfaces with different length scales are generically referred to as Frenkel-
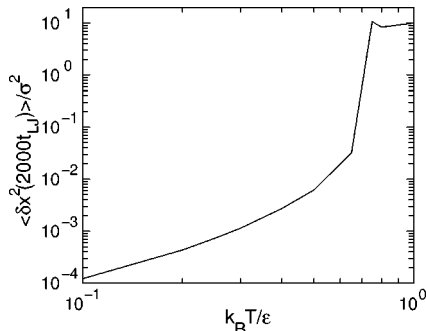

FIG. 5. Mean-squared displacement of top wall along a single coordinate, $\langle \delta x^2(t) \rangle$, after time $t = 2000_{LJ}$ as a function of T at $f_z = 0.75 \epsilon/\sigma$. The walls are commensurate and $N = 32 \times 32$.
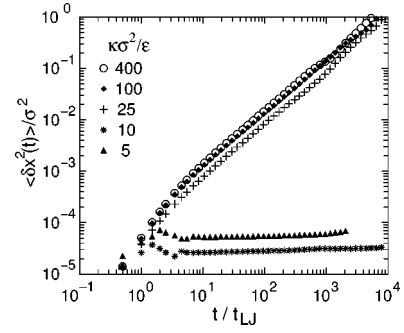

FIG. 6. Mean-squared displacement of top wall along a single coordinate, $\langle \delta x^2(t) \rangle$, as a function of time t for different couplings κ of wall atoms to their equilibrium positions. Here $k_B T = 0.1 \epsilon$, $f_z = 0.1 \epsilon/\sigma$, and $r_c = 2.2 \sigma$. The walls are incommensurate and $N = 31 \times 36$.

Kontorova (FK) models and many examples have been studied.[12,13] In the limit of infinite, perfectly rigid walls it can be shown that the free energy barrier for sliding motion is exactly zero if the walls are incommensurate.[12,13] Thus the top wall will diffuse freely in the thermodynamic limit. Finite systems with periodic boundary conditions, like those considered here, can never be perfectly incommensurate. The order of commensurability can be measured by the smallest integer q that allows the ratio of lattice constants to be expressed as p/q, where p is also an integer. Theoretical calculations[13,23] suggest that ΔF vanishes exponentially fast with increasing q. If the highest possible value of q is chosen for each system size, then the total value of ΔF should vanish in the thermodynamic limit at least as fast as $c_1 N \exp(-\sqrt{c_2 N})$, where the c_i are constants. Thus our simulations should show the same behavior as truly incommensurate systems in the thermodynamic limit.

As the constraint of perfect rigidity is relaxed, it becomes possible for two incommensurate walls to lock into a common periodicity.[12,13] There is a transition at a critical value of the ratio of the strength of the intersurface potential to the internal stiffness of the walls. This would correspond to the ratio $\Delta F / N \sigma^2 \kappa$ in our simulations. The critical value depends on the shape of the potential and the ratio of lattice constants, and has mostly been determined for one-dimensional systems.

To illustrate this behavior we consider two incommensurate walls of size 31×36 atoms and vary the wall stiffness κ. One wall is rotated by 90° with respect to the other wall. Then small strains are applied to make the resulting surfaces square so that they share the same periodic boundary conditions. Unlike the other simulations presented here, we use a long cutoff radius, $r_c = 2.2 \sigma$, for the Lennard-Jones potential between atoms on different walls. One consequence of this is that there is an effective normal force on each atom due to the adhesion of the surfaces that is of order ϵ/σ. We used a small external force $f_z = 0.1 \epsilon/\sigma$ and a low temperature $k_B T = 0.1 \epsilon$ so that thermal fluctuations are small.

In Fig. 6, the mean-squared displacement of the top wall is plotted against time. For $\kappa \lesssim 10 \epsilon/\sigma^2$ the top wall is pinned and the mean-squared displacement saturates at a very small fraction of a lattice constant. Direct observations of atomic positions show that atoms have undergone large rearrangements from their initial lattice sites in order to lock together
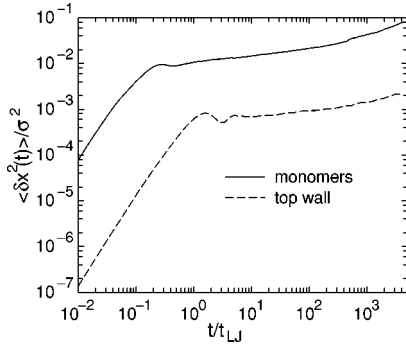
FIG. 7. Mean-squared displacement along a single coordinate, $\langle \delta x^2(t) \rangle$, of individual monomers and of top wall as a function of time t at $k_B T = 0.8\epsilon$ and $f_z = 10\epsilon/\sigma$ for incommensurate walls with $N = 31 \times 36$.

in a free energy minimum. For all $\kappa \geq 25\epsilon/\sigma^2$, the walls follow nearly identical curves, and the asymptotic behavior is consistent with the free diffusion constant D_0. Note that there is a smooth crossover from ballistic to diffusive motion with no subdiffusive regime like that found for monomers between commensurate walls (Fig. 3). This indicates that there is no potential well that temporarily locks the surfaces together.[21] Our results for commensurate systems show that the above findings are not enough for us to conclude that the top wall would remain depinned in the thermodynamic limit at $\kappa \geq 25\epsilon/\sigma^2$. However, in contrast to the commensurate systems, increasing the system size does not change the value of κ where the transition occurs. If there was a finite ΔF that scaled with N this shift would be evident.

We can use the Lindemann criterion to estimate what κ should be in order to model a Lennard-Jones crystal. In order to have an rms displacement of 10% of the nearest-neighbor spacing at the triple point ($k_B T = 0.7\epsilon$), we must have $\kappa \approx 140\epsilon/\sigma^2$. This is well into the range of values where we find free diffusion. In order to see pinning for realistic values of κ, the interaction between the walls must be increased relative to that within the walls (i.e., κ). This can be done by increasing the normal force.

Note that our use of springs connected to lattice sites is an Einstein approximation to an elastic crystal and does not treat long-wavelength elastic deformations accurately. However, the displacements required to lock two lattices together have relatively short wavelengths, and simulations with more accurate elastic models yield the same transition from depinned to pinned with an increasing ratio between the strength of inter- and intrawall interactions.[12,13]

2. Submonolayer lubrication

As above, two identical walls were made incommensurate by a rotation of 90°, and then strained slightly to fit square periodic boundary conditions. As for the commensurate case, the film contained about 1 monomer for every 4 atoms in each wall layer or about 1/4 of a monolayer. Unless otherwise noted, the walls contained 31×36 atoms each, and there were 46 film molecules containing six monomers each. We chose to consider the most difficult case for pinning bare surfaces, completely rigid walls ($\kappa = \infty$).

We first compare the diffusion of the top wall to that of individual monomers. Figure 7 shows results for the same
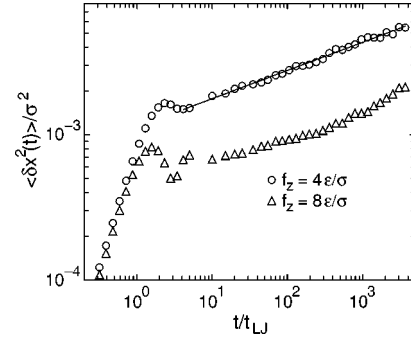

FIG. 8. Mean-squared displacement of top wall along a single coordinate, $\langle \delta x^2(t) \rangle$, as a function of time t for two different normal forces and $k_B T = 0.8\epsilon$. Bottom and top wall are incommensurate and $N = 31 \times 36$. The straight line is a fit to a power law t^α with $\alpha = 0.194 \pm 0.004$.

parameters ($f_z = 10\epsilon/\sigma$, $k_B T = 0.8\epsilon$) as the commensurate system of Fig. 3. Note that individual monomers are much less mobile at long times when between the incommensurate walls. Presumably this is because commensurate walls produce long channels of relatively wide openings between parallel lines of atoms on opposing walls. Incommensurate walls produce a more random environment with fewer large openings between atoms on opposing walls.

The incommensurate walls themselves move further and more rapidly than commensurate walls. As a result there is no clear time separation between the motion of monomers and walls in the incommensurate case at this N. Over the time interval shown the top wall appears pinned, because the motion is subdiffusive, and the total distance moved is less than 10% of a lattice constant. The monomers have also moved less than a lattice constant and exhibit subdiffusive motion.

Figure 8 shows how the diffusion of the top wall changes with decreasing normal force. As in Fig. 7 the walls move ballistically up to a time $t \approx 1$. The distance traversed increases as f_z decreases. At longer times, motion is subdiffusive and the curves are roughly parallel on a log-log plot. For $f_z = 4$, the mean-squared displacement can be described by a power law $\langle \delta x^2(t) \rangle \propto t^\alpha$, for at least three decades of time. An exponent of $\alpha = 0.194 \pm 0.004$ is obtained.

As in the commensurate case, there appears to be a transition from pinned to depinned as f_z decreases or T increases. Figures 9 and 10 show the mean-squared displace-
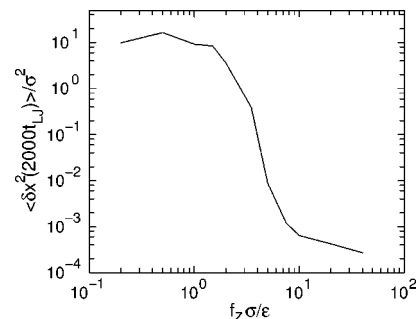

FIG. 9. Mean-squared displacement of top wall along a single coordinate, $\langle \delta x^2(t) \rangle$, after time $t = 2000\, t_{LJ}$ as a function of f_z at $k_B T = 0.8\epsilon$. The walls are incommensurate and $N = 31 \times 36$.
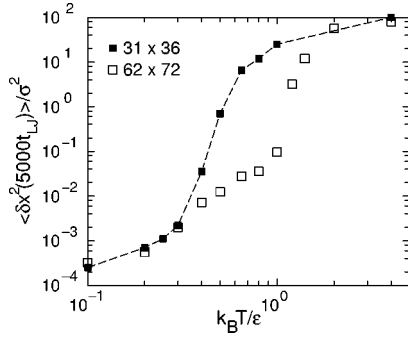
FIG. 10. Mean-squared displacement of top wall along a single coordinate, $\langle \delta x^2(t) \rangle$, after time $t = 5000\,t_{LJ}$ as a function of temperature for two different system sizes at $f_z = 2\epsilon/\sigma$. The results for the larger wall were multiplied by a factor of four to remove the trivial dependence on wall mass.

ment after $2000 t_{LJ}$ as a function of f_z and T, respectively. Note that the displacement changes over a somewhat broader range than in the corresponding figures for the commensurate walls (Figs. 4 and 5). The transition is also at a lower T and higher f_z, indicating that it is more difficult to pin the incommensurate walls. This is consistent with our studies of the static friction,[14] which is roughly proportional to ΔF. We found that submonolayer films between commensurate walls gave three to five times larger friction forces than incommensurate walls under similar conditions.[14]

To test whether the transition from pinned to depinned is real, we performed simulations with larger walls at the same film density. Figure 11 compares results for walls containing 31×36 atoms and 62×72 atoms at $f_z = 2\epsilon/\sigma$ and $k_B T = 0.8\epsilon$. Note that the monomer diffusion is nearly identical at the two system sizes, and shows a clear diffusive region (slope of one) at the longest times. This implies that the energy landscape that monomers move through is not influenced by system size. In contrast, there is a striking size dependence in the dynamics of the top wall. The trivial size dependence of the free diffusion constant, $D_0 \propto N$, has been removed by multiplying the mean-squared displacement of the larger wall by four. This collapses results for different sizes in the ballistic regime ($t < 10 t_{LJ}$). At larger times the
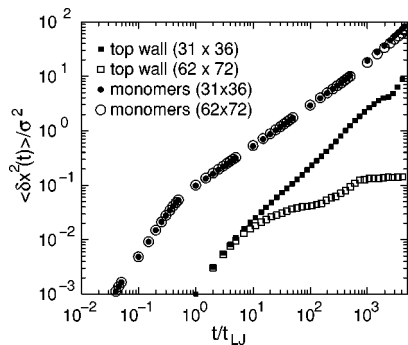

FIG. 11. Mean-squared displacement along a single coordinate, $\langle \delta x^2(t) \rangle$, for the top wall (squares) and monomers (circles) at two different system sizes with $f_z = 2\epsilon/\sigma$ and $k_B T = 0.8\epsilon$. The mean-square displacement of the larger top wall has been multiplied by a factor of four to be compatible with the small system in the ballistic regime, and the larger system contained four times as many film molecules (184).

smaller wall shows a simple crossover from ballistic to diffusive motion, while the larger wall shows subdiffusive behavior and seems to stop moving at long times. (The step in the data at a few hundred t_{LJ} is a result of a rare, relatively large displacement of the wall.) This is the same type of behavior that was seen for increasing system size in commensurate systems. It indicates that there is a finite ΔF that grows with N causing motion to stop as $N \Delta F$ rises above $k_B T$. One can conclude that the incommensurate walls are pinned in the thermodynamic limit for these parameters.

The apparent transition between pinned and depinned states continues to shift to higher T (Fig. 10) and lower f_z with increasing N for the largest systems we have been able to study. However, we have no analog of the argument for commensurate walls that suggests that incommensurate walls should be pinned at all T and f_z. The density modulation produced by one wall will be incommensurate with the opposite wall and produce no net energy shift. Locking between the two surfaces must enter as a higher-order susceptibility that is difficult to calculate. For $f_z \ll k_B T/\sigma$ the walls move far apart and the molecules form an increasingly ideal gas. It seems reasonable that the depinning force would vanish in the thermodynamic limit under these conditions, but this remains an open question.

IV. CONCLUSIONS

We have performed a systematic study of the conditions for pinning of commensurate and incommensurate walls. The case of bare walls is relatively straightforward and has been considered previously. However, examination of the scaling of the diffusion with system size N, temperature T, and normal force f_z provides a useful benchmark for our studies of submonolayer films. Bare commensurate walls are always pinned by a periodic potential that grows with system size. However, relatively large systems can appear unpinned if the potential is small enough. Incommensurate walls are completely unpinned until they become so deformable that they can rearrange by distances of order σ to accommodate the opposing wall.

Commensurate walls remain pinned when a submonolayer film is introduced between them. A general argument was given that this pinning should always exist, and our results show that even when the film becomes a gas the walls do not diffuse in the thermodynamic limit. However, the pinning is very weak and one has to go to large system sizes to detect it. Curry and coworkers have also seen pinning of commensurate walls by diffusing films.[6]

Introducing a submonolayer film can pin incommensurate walls, even when they are completely rigid. In the Introduction we noted that diffusion of a monomer to an inequivalent site should cause a displacement of the top wall in any finite system, and wondered whether such displacements might accumulate into diffusion of the top wall. However, the monomer will in general diffuse to a site that minimizes its energy for the given position of the top wall, and thus add to the potential energy barrier that pins it. Our results are consistent with a pinning potential that is linear in N, just as in the commensurate case. Independent studies of the static friction as a function of system size confirm this linear relation.[14]

The behavior of incommensurate walls in the thermody-

namic limit is very important to the study of static friction, since contacting surfaces are almost never commensurate. Our studies confirm previous work[12,13] in showing that bare incommensurate walls are very unlikely to exhibit static friction in the thermodynamic limit. Surfaces are also very unlikely to be bare, especially if exposed to air. Our results clearly show that even a small fraction of a monolayer between the surfaces is enough to produce static friction in the thermodynamic limit. A particularly surprising result is that the monolayer itself need not be in a crystalline or glassy state. As shown in Fig. 11, molecules may undergo nearly unhindered diffusion and still produce static friction over large enough areas. It remains to be seen whether there is a transition to a depinned state as the layer is made thicker by lowering pressure, increasing temperature, or introducing more molecules between the surfaces.

---

[1] M. Schoen, C. L. Rhykerd, D. J. Diestler, and J. H. Cushman, Science **245**, 1223 (1989); C. L. Rhykerd, M. Schoen, D. J. Diestler, and J. H. Cushman, Nature (London) **330**, 461 (1987).

[2] P. A. Thompson and M. O. Robbins, Science **250**, 792 (1990).

[3] P. A. Thompson, G. S. Grest, and M. O. Robbins, Phys. Rev. Lett. **68**, 3448 (1992); P. A. Thompson, M. O. Robbins, and G. S. Grest, Isr. J. Chem. **35**, 93 (1995).

[4] J. P. Gao, W. D. Luedtke, and U. Landman, Phys. Rev. Lett. **79**, 705 (1997).

[5] E. Manias, G. Hadziiaoannou, and G. ten Brinke, J. Chem. Phys. **101**, 1721 (1994).

[6] J. E. Curry, F. Zhang, J. H. Cushman, M. Schoen, and D. J. Diestler, J. Chem. Phys. **101**, 10 824 (1994).

[7] J. Israelachvili, P. M. McGuiggan, and A. M. Homola, Science **240**, 189 (1988); M. L. Gee, P. M. McGuiggan, J. N. Israelachvili, and A. M. Homola, J. Chem. Phys. **93**, 1895 (1990); A. M. Homola, J. N. Israelachvili, P. M. McGuiggan, and M. L. Gee, Wear **136**, 65 (1990).

[8] J. Van Alsten and S. Granick, Phys. Rev. Lett. **61**, 2570 (1988); Langmuir **6**, 876 (1990).

[9] A. L. Demirel and S. Granick, Phys. Rev. Lett. **77**, 2261 (1996).

[10] J. Klein and E. Kumacheva, Science **269**, 816 (1995); J. Chem. Phys. **108**, 6996 (1998).

[11] M. Lupowski and F. van Swol, J. Chem. Phys. **95**, 1995 (1991); B. N. J. Persson and A. Nitzan, Surf. Sci. **367**, 261 (1996).

[12] Y. I. Frenkel and T. Kontorova, Zh. Eksp. Teor. Fiz. **8**, 1340 (1938); S. Aubry, Physica D **7**, 240 (1983); P. Bak, Rep. Prog. Phys. **45**, 587 (1982); K. Shinjo and M. Hirano, Surf. Sci. **283**, 473 (1993).

[13] M. Weiss and F. J. Elmer, Phys. Rev. B **53**, 7539 (1996).

[14] G. He, M. H. Müser, and M. O. Robbins, Science **284**, 1650 (1999).

[15] K. Kremer and G. S. Grest, J. Chem. Phys. **92**, 5057 (1990).

[16] P. Hänggi, P. Talkner, and M. Borkovec, Rev. Mod. Phys. **62**, 251 (1990).

[17] G. S. Grest and K. Kremer, Phys. Rev. A **33**, 3628 (1986).

[18] V. Ambegaokar and B. I. Halperin, Phys. Rev. Lett. **22**, 1364 (1969).

[19] H. Risken and H. D. Vollmer, Z. Phys. B **33**, 297 (1979), and references therein.

[20] M. D. Perry and J. A. Harrison, J. Phys. Chem. B **101**, 1364 (1997); Thin Solid Films **290**, 211 (1996).

[21] K. Kremer, G. S. Grest, and M. O. Robbins, J. Phys. A **20**, L181 (1987); *Anomalous Diffusion*, edited by R. Kutner, A. Pekalski, and Sznajd-Weron (Springer, Berlin, 1999).

[22] C. Heinbuch and J. Fischer, Phys. Rev. A **40**, 1144 (1989); P. A. Thompson and M. O. Robbins, *ibid.* **41**, 6830 (1990); M. Cieplak, E. D. Smith, and M. O. Robbins, Science **265**, 1209 (1994).

[23] M. H. Müser, L. Wenning, and M. O. Robbins (unpublished).